Journal of Electrostatics 102 (2019) 103377

Contents lists available at ScienceDirect

Journal of Electrostatics

journal homepage: http://www.elsevier.com/locate/elstat

Non-Coulombic behavior of electrostatic charge-charge interaction in three-layer heterostructures

Alexander M. Gabovich [a,*], Mai Suan Li [b], Henryk Szymczak [b], Alexander I. Voitenko [a]

[a] Institute of Physics, National Academy of Sciences of Ukraine, 46, Nauka Ave., Kyiv, 03680, Ukraine
[b] Institute of Physics, Polish Academy of Sciences, 32/46, Al. Lotników, PL-02-668, Warsaw, Poland

ARTICLE INFO

Keywords:
Three-layer structures
Electrostatic interaction
Polarization forces
Non-Coulombic dependence

ABSTRACT

Electrostatic interaction energy $W_{Q_1Q_2}$ between two point charges Q_1 and Q_2 in a three-layer planar system was calculated on the basis of the Green's function method in the classical electrostatic model with constant dielectric permittivities ε_i ($i = 1, 2, 3$) for all constituent media. Two significant particular cases of charge configurations were analyzed in more detail: (i) when the both charges are in the same medium and their perpendicular coordinates are equal, $Z_1 = Z_2$, and (ii) the charges are located at different interfaces and interact across the slab. It was demonstrated that the $W_{Q_1Q_2}$ dependences on the charge-charge distance S and its projection R on the XY plane [$S^2 = R^2 + (Z_1 - Z_2)^2$] differ from the classical Coulombic one. This phenomenon occurs due to the appearance of polarization charges at both interfaces, making the problem a many-body one. Numerical calculations demonstrated that both the underscreening and overscreening of the electrostatic charge-charge interaction is possible depending on the charge arrangement and the relationships between ε_i's in the layers. The deviations from the Coulomb law were found to be especially large when the dielectric constants of the covers are much larger or much smaller than that in the interlayer.

1. Introduction

Owing to its ubiquity and long-range character, the proper account of the electrostatic charge-charge interaction in inhomogeneous systems is very important for the correct description of their properties. Indeed, electrons and holes in semiconductor heterostructures [1–9] or metal-oxide-semiconductor structures [10,11], as well as two-dimensional (2D) electron sheets above thin films of cryogenic liquids [12–15], constitute charged liquids, which properties crucially depend on the properties of the electrostatic interaction between the charges screened by all the media involved. In this connection, it is no wonder that the problem of electrostatic interaction in structures with inhomogeneous screening properties has been extensively studied in the past [16–29]. Nevertheless, a very important aspect of the general problem has been overlooked. To be specific, the classic Coulomb dependence

$$W = C\frac{Q_1 Q_2}{S}, \tag{1}$$

where C = const, was rather often applied to model the electrostatic interaction W between charges Q_1 and Q_2 located in the *heterogeneous* environment and separated by the distance S. No proper comprehensive analysis of the Coulomb law violation in various corresponding structures has been done until now, although the origin and importance of the screening inhomogeneity is well recognized ever since the polarization forces at medium interfaces have been theoretically discovered [30–32].

In essence. we have a difference between the description of electrostatic field at the micro- and macroscopic levels. Really, dependence (1) obeys the equation

$$\Delta W = 0, \tag{2}$$

where Δ is the Laplace operator. For Eq. (2) to adequately describe the electrostatic interaction between two point charges, the medium where the charges are located must be homogeneous. This condition can be satisfied rather well at microscopic distances between the charges. But at the physically "macroscopic" scale (which is actually microscopic from the truly macro-scale point of view!), when the microscopic Maxwell equations should be averaged over the so-called "physically small"

* Corresponding author.
E-mail addresses: gabovich@iop.kiev.ua (A.M. Gabovich), masli@ifpan.edu.pl (M.S. Li), szymh@ifpan.edu.pl (H. Szymczak), voitenko@iop.kiev.ua (A.I. Voitenko).

https://doi.org/10.1016/j.elstat.2019.103377
Received 30 July 2019; Received in revised form 30 September 2019; Accepted 3 October 2019

volumes, the situation changes [32,33].

For instance, in the case when the charges in the medium are free, they are redistributed under the action of the source (in particular, a point charge) electric field. In the linearized (Thomas-Fermi or Debye) approximation, the resulting equation for the microscopically averaged charge potential in an otherwise homogeneous medium has the form

$$\Delta\phi - \kappa^2\phi = 0, \tag{3}$$

where κ is the inverse screening length. Then, the interaction energy between charges Q_1 and Q_2 looks like

$$W = C\frac{Q_1Q_2}{S}\exp(-\kappa S). \tag{4}$$

As a result, Eq. (2), as well as the Coulombic law (1), becomes no more valid at the macroscopic level.

However, the validity of Eq. (2) does not guarantee that the interaction of a charge with a system of charges in a homogeneous medium is described by dependence (1). The simplest example is the interaction of the charge Q_1 with two other charges Q and Q', which are considered as a single object. The resulting sum

$$C\frac{Q_1Q}{S_1} + C\frac{Q_1Q'}{S_2}$$

cannot be presented in form (1). Thus, being beyond the scope of the two-body problem leads to the immediate violation of the Coulombic dependence (1). This is quite trivial, and the Coulombic contribution of any charge can isolated. However, the existence of interfaces between areas with different dielectric constants makes the problem inevitably a many-body one, since the pair of charges Q_1 and Q_2 induces mutually independent (the Maxwell and constitutive equations are linear!) continuous polarization charge distributions at those interfaces. Of course, the same conclusion should be made if the probe charges are non-point-like ones [32].

We have already carried out a relevant analysis of the Coulomb law violation for the two-layer system of classic insulators [34]. But, for the three-layer system, the problem becomes much more intricate due to the interference of electrostatic fields created by polarization charges located at different interfaces [28,31]. As a result, it goes beyond the scope of the elementary approach and requires more sophisticated techniques (in our case, this is the Green's function method [16,20,25,35]).

A comprehensive consideration of the classical electrostatic interaction energy W in three-layer structures was carried out in [36]. Here, on the basis of the results obtained in the cited work, we estimate the applicability of dependence (1) in those systems. The consideration is carried out for two (from our viewpoint, the most interesting) arrangements of charges: at the same distance from the interfaces and at different interfaces. The latter arrangement is important, e.g., for excitons in heterostructures [9,37–43] or monolayers [44–46] and possible electron-hole superfluidity [47–55]. The results obtained show that, similarly to the case of two media [34], the polarization charges at the interfaces really violate the Coulombic dependence (1) of W on the distance S between the charges. i. e. the quantity W is no longer proportional to S^{-1}. Instead, in some cases, it is reasonable to approximate the actual $W(S)$ behavior by the dependence

$$W = C\frac{Q_1Q_2}{S^N}. \tag{5}$$

Both the coefficient C and the effective power exponent N in this formula turn out to be weak functions of S. Nevertheless, we demonstrate that those parameters can be regarded as constants in rather large S-intervals.

The structure of the paper is as follows. In section 2, for completeness, we formulate the problem of calculating W in the three-layer system and describe the method to calculate the effective power exponent in approximation (5). In two next sections, we separately consider the charge arrangements indicated above.

2. Theoretical part

2.1. Formulation of the three-layer problem

Two point-like charges Q_1 and Q_2 are considered to be located in a three-layer system (Fig. 1). Two semi-infinite covers (media 1 and 3) are separated by a flat slab (medium 2) of the thickness L. All three media in electrostatics are characterized by the dielectric functions $\varepsilon_i(\mathbf{k})$, $i = 1, 2, 3$, which, in principle, depend on the transferred wave vector $\mathbf{k}$ (the spatial dispersion of the dielectric functions). The central plane of the slab is identified with the XY plane. The charge coordinates Z_1 and Z_2 are reckoned from this plane, so that $(Z_1, Z_2) < -L/2$ in medium 1, $-L/2 < (Z_1, Z_2) < L/2$ in medium 2, and $(Z_1, Z_2) > L/2$ in medium 3. The longitudinal (along the XY plane) distance between the charge projections equals R, so that the actual distance is

$$S = \sqrt{R^2 + (Z_1 - Z_2)^2}. \tag{6}$$

The explicit expressions describing the charge-charge interaction energy $W(S)$ in a three-layer structure for the general case of the spatial dispersion of dielectric permittivities can be found using any of several equivalent approaches [20,25,27,28]. They are based on the assumptions of the infinite interface barriers and the specular reflection of charge carriers at the interfaces [19,56–63]. As a result, the energy $W(S)$ can be presented in the form

$$W_{ij}(R, Z_1, Z_2) = -2Q_1Q_2\int_0^\infty qdqD_{ij}(q, Z_1, Z_2)J_0(qR), \tag{7}$$

where the subscripts i and j denote the media where the charges Q_1 and Q_2, respectively, are located; and $J_0(x)$ is the Bessel function of the first kind. The functions

$$D_{ij} = \frac{A_i(Z_1)B_j(Z_2) + \tilde{A}_i(Z_1)\tilde{B}_j(Z_2)}{C} - F_i(Z_1, Z_2)\delta_{ij}, \tag{8}$$

where δ_{ij} is the Kronecker delta, were called Green's functions of the three-layer Coulomb problem [16]. They describe the screened electrostatic interaction and allow both the charge-charge interaction and the self-energy of the charge in the layered system (the image charge energy [20,25,28]) to be calculated.

The expressions entering Eq. (8) are

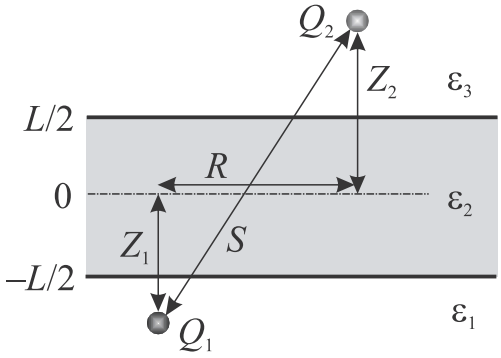

Fig. 1. Layout of the problem. Point charges Q_1 and Q_2 in a three-layer structure with the dielectric permittivities ε_i ($i = 1, 2, 3$) of the media separated by plane interfaces at $Z = \pm L/2$. The perpendicular co-ordinates of the charges are Z_1 and Z_2 reckoned from the central plane $Z = 0$. S is the distance between the charges, and R is the longitudinal (along the XY plane) distance between their projections.

$$A_1(Z_1) = \tilde{A}_1(Z_1) = a_1\left(Z_1 + \frac{L}{2}\right),$$

$$A_2(Z_1) = -a_S(Z_1), \quad \tilde{A}_2(Z_1) = -a_A(Z_1),$$

$$A_3(Z_1) = -\tilde{A}_3(Z_1) = a_3\left(Z_1 - \frac{L}{2}\right),$$

$$B_1(Z_2) = a_1\left(Z_2 + \frac{L}{2}\right)[a_A(0) + a_3(0)],$$

$$\tilde{B}_1(Z_2) = a_1\left(Z_2 + \frac{L}{2}\right)[a_S(0) + a_3(0)],$$

$$B_2(Z_2) = -\frac{1}{2}\{[a_S(Z_2) + a_A(Z_2)][a_A(0) + a_3(0)] + [a_S(Z_2) - a_A(Z_2)][a_A(0) + a_1(0)]\},$$

$$\tilde{B}_2(Z_2) = -\frac{1}{2}\{[a_S(Z_2) + a_A(Z_2)][a_S(0) + a_3(0)] - [a_S(Z_2) - a_A(Z_2)][a_S(0) + a_1(0)]\},$$

$$B_3(Z_2) = a_3\left(Z_2 - \frac{L}{2}\right)[a_A(0) + a_1(0)],$$

$$\tilde{B}_3(Z_2) = -a_3\left(Z_2 - \frac{L}{2}\right)[a_S(0) + a_1(0)],$$

$$C = [a_S(0) + a_1(0)][a_A(0) + a_3(0)] + [a_S(0) + a_3(0)][a_A(0) + a_1(0)],$$

$$F_1(Z_1, Z_2) = b_1(Z_1, Z_2),$$

$$F_2(Z_1, Z_2) = \frac{1}{2}[b_S(Z_1, Z_2) + b_A(Z_1, Z_2)],$$

$$F_3(Z_1, Z_2) = b_3(Z_1, Z_2),$$

where

$$a_{1,3}(Z) = \frac{1}{\pi}\int_{-\infty}^{+\infty} \frac{dk_\perp \cos k_\perp\left(Z \pm \frac{L}{2}\right)}{(k_\perp^2 + q^2)\varepsilon_{1,3}(\mathbf{q}, k_\perp)}, \tag{9}$$

$$a_{S,A}(Z) = \frac{2}{L}\sum_{k_\perp^{S,A}} \frac{\exp(ik_\perp Z)}{(k_\perp^2 + q^2)\varepsilon_2(\mathbf{q}, k_\perp)}, \tag{10}$$

$\mathbf{q}$ and $k_\perp$ are the longitudinal (along the interfaces) and perpendicular (to the interfaces), respectively, components of the wave vector $\mathbf{k}$,

$$k_\perp^S = \frac{2n\pi}{L}, \quad k_\perp^A = \frac{(2n+1)\pi}{L} \quad (n = 0, \pm1, \pm2, \ldots),$$

$$b_1(Z_1, Z_2) = \frac{1}{2}\{a_1(Z_1 + Z_2 + L) + a_1(Z_1 - Z_2)\},$$

$$b_{S,A}(Z_1, Z_2) = \frac{1}{2}[a_{S,A}(Z_1 + Z_2 + L) + a_{S,A}(Z_1 - Z_2)], \tag{11}$$

$$b_3(Z_1, Z_2) = \frac{1}{2}\left\{a_3\left(\left|Z_1 - \frac{L}{2}\right| + \left|Z_2 - \frac{L}{2}\right|\right) + a_3\left(\left|Z_1 - \frac{L}{2}\right| - \left|Z_2 - \frac{L}{2}\right|\right)\right\}.$$

Hereafter, we restrict the analysis to the classical case of dispersionless dielectric constants $\varepsilon_i = \text{const}$, $i = 1, 2, 3$. Then, the quantities $a_{1,3,S,A}(Z)$ can be integrated analytically:

$$a_{1,3}(Z) = \frac{1}{\varepsilon_{1,3} q}\exp\left(-q\left|Z \pm \frac{L}{2}\right|\right), \tag{12}$$

$$a_S\left(-\frac{L}{2} \le Z \le \frac{L}{2}\right) = \frac{1}{q\varepsilon_2}\frac{\cosh(qZ)}{\sinh\left(\frac{qL}{2}\right)}, \tag{13}$$

$$a_A\left(-\frac{L}{2} \le Z \le \frac{L}{2}\right) = -\frac{1}{q\varepsilon_2}\frac{\sinh(qZ)}{\cosh\left(\frac{qL}{2}\right)}. \tag{14}$$

If the argument Z extends beyond the specified limits, the functions $a_{S,A}(Z)$ should be recalculated as follows:

$$a_S(Z) = a_S(Z \pm L),$$

$$a_A(Z) = -a_A(Z \pm L).$$

2.2. Where is the Coulombic behavior obeyed?

The results of [36] demonstrate that, in the case of a three-layer system composed of dispersionless insulators with different dielectric permittivities ($\varepsilon_1 \neq \varepsilon_2 \neq \varepsilon_3$), the functional dependence (1) between the quantities W and S can be achieved only in the following limiting cases.

(i) The point charges are located in the same medium ($i = 1, 2, 3$) infinitesimally close to each other ($S \to 0$), so that their distances to the interfaces become much larger. The contribution of direct Coulombic interaction prevails, and the charges "cease to feel" both the interfaces and the polarization charges induced at them. In this case, the proportionality coefficient C in formula (1) equals ε_i^{-1}.

(ii) The charges are located infinitesimally close to each other and are located at the interface between the i-th and j-th media or across this interface, which is equivalent to "at the interface" for infinitesimally close charges: $S \to 0$, $(Z_1, Z_2) \to L/2 \pm 0$. The corresponding proportionality coefficient C equals $2/(\varepsilon_i + \varepsilon_j)$. In this case, the charges "cease to feel" the other interface, and the problem acquires a two-layer character. Therefore, owing to the problem symmetry, if the both charges are positioned at the interface, the electric field vector is directed along the interface, and there are no polarization charges at this interface.

(iii) The both charges are in the same cover ($i = 1, 3$), at a finite distance from each other, but infinitely far from the both interfaces: $(S, L) \ll (|Z_1|, |Z_2|)$. The proportionality coefficient C evidently equals ε_1 in medium 1 and ε_3 in medium 3. In essence, this is a reformulated version of case (i) when $L \to 0$.

(iv) The charges are rather close to the interfaces, but far from each other longitudinally: $R \gg (|Z_1|, |Z_2|, L)$. The proportionality coefficient C equals $2/(\varepsilon_1 + \varepsilon_3)$ irrespective in which media the charges are located. This is a reformulated version of case (ii) when $(L, Z_1, Z_2) \to 0$. The slab effectively becomes infinitesimally narrow, and the three-layer problem transforms into the two-layer one (media 1 and 3 separated by a plane interface).

It is easy to understand that in all indicated cases, the contribution to the interaction energy W of polarization charges emerging at the interfaces vanishes.

Thus, we have six (in the general case) different values of the coefficient C in asymptotics (1): one value

$$C = \frac{2}{\varepsilon_1 + \varepsilon_3} \tag{15}$$

for $S \to \infty$, and five values

$$C = \frac{1}{\varepsilon_1}, \frac{2}{\varepsilon_1 + \varepsilon_2}, \frac{1}{\varepsilon_2}, \frac{2}{\varepsilon_2 + \varepsilon_3}, \frac{1}{\varepsilon_3} \tag{16}$$

for $S \to 0$. When crossing the interfaces, the coefficient C changes

abruptly at each interface. More precisely, each modification involves two jumps: from ε_i^{-1} in the i-th medium to $2/(\varepsilon_i+\varepsilon_j)$ at the interface and further to ε_j^{-1} in the j-th medium. Note that the abrupt jumps are a consequence of the assumed infinitely thin interfaces between the media involved. If a realistic smooth transition between the media is taken into account, the polarization (image force) energy does not diverge at the interfaces [64]. Therefore, in this case, the jumps of C will be smeared as well. Unfortunately, for smeared interfaces, the whole problem becomes extremely cumbersome and goes far beyond our purposes. Anyway, dependence (1) with a single $C = \text{const}$ evidently cannot simultaneously satisfy the specified asymptotics, and the violation of the Coulombic law even in the simplest dispersionless three-layer system becomes a matter of fact. Then, one may ask the following questions:

(A) To what extent formula (1) is sufficient for the description of charge interaction in the three-layer system?
(B) If it works badly, can the generalized Coulomb-like power-law formula (5) with $N \neq 1$ be used for this purpose?

It should be clear at this stage, that the parameters C and N in both formulas cannot be constant, but they depend on other problem parameters: Z_1, Z_2, L, and R. In both cases, it is desirable to find S-intervals where the indicated approximation formulas are applicable.

2.3. Apparent power exponent

To reduce the number of problem parameters, let us normalize all length-related quantities—these are L, R, S, Z_1, and Z_2—by the characteristic length of the problem, the interlayer width L, which does not depend on the charge positions. The corresponding dimensionless quantities will be designated by the same letters, but in the lower case; i.e. r, s, z_1, and z_2. The interaction energy W can also be reduced to the dimensionless quantity w:

$$W = \frac{Q_1 Q_2}{L} w. \tag{17}$$

We also note that from the theoretical and experimental viewpoints, it is more convenient to examine the dependence $w(r)$ rather than $w(s)$.

From the aforesaid, it is clear that the product sw is a good criterion of the true Coulombic behavior of the dependence $w(s)$: this product must be constant within the intervals where this law is obeyed. This criterion was used in [36], and we found that it is obeyed almost nowhere (see section 2.2).

Another way consists in the evaluation of the parameter N itself. For further consideration, let us change the sign of power exponent N in formula (5). Hence, let us suppose that, in the vicinity of any distance s_0 between two point charges, the formula describing the electrostatic interaction between them can be expressed in the form

$$w(s) \approx C(s_0) s^{N(s_0)}. \tag{18}$$

Actually, this means an expansion of the $w(s)$ dependence in a non-integer-power series of s retaining the leading term only. Then, one obtains

$$N(s) = s \frac{d}{ds} \ln w = \frac{s}{w} \frac{dw}{ds}. \tag{19}$$

For the genuine Coulombic dependence $w \tilde{} s^{-1}$, formula (19) gives $N = -1$.

The quantity w (see section 2.1) cannot be presented in a finite analytical form including elementary and/or special functions. In [36], we developed a regular method, in which integral (7) is calculated as a convergent series of terms like

$$\frac{A}{\sqrt{r^2 + (z_1 \pm z_2 + B)^2}} = \frac{A}{\sqrt{s^2 - (z_1 - z_2)^2 + (z_1 \pm z_2 + B)^2}}, \tag{20}$$

where A and B are coefficients specific for every term, which depend on the $\{\varepsilon_i\}$ set and on the layer in which the point is located. The method allows the magnitude of w to be calculated with any given accuracy. But the convergence rate of the series is different at different points. Therefore, the number of terms to be summed up is also different and can be rather large. As a result, there is no finite analytical formula for the calculation of w. At the same time, the derivative of term (20) with respect to r (or s) is obvious. Therefore, the calculation procedure consists in that the analytical series for $w(r)$ and $dw(r)/ds$ are accumulated in parallel at every r with a simultaneous monitoring of the numerical accuracy for w. When a desired relative accuracy for w is attained (as a rule, it is 10^{-4}), the calculation is terminated, and the obtained w- and dw/ds-expressions are substituted into formula (19) for the numerical evaluation.

3. The case of equivalently located charges $z_1 = z_2$

Let us first consider the case, when the both charges are positioned at the same vertical level ($z_1 = z_2 \equiv z$) in the three-layer system. Then, the normalized distance s between them [see Eq. (6)] becomes equal to the parameter r, which describes their relative interval in the lateral plane (see Fig. 1). In particular, the criterion sw transforms into rw. Formula (19) now reads

$$N(r) = \frac{r}{w} \frac{dw}{dr}. \tag{21}$$

3.1. Non-symmetric structures

Fig. 2 demonstrates the dependences of the product rw on the lateral (and actual!) distance r between the charges with various $z_1 = z_2$ coordinates for a toy three-layer structure with $\{\varepsilon_i\} = 1:2:5$. This is one of the $\{\varepsilon_i\}$-combinations at which the $rw(r)$ profiles do not intersect one another, so that various peculiarities in their behavior can be clearly compared. It is evident at once that the constancy of the product rw is

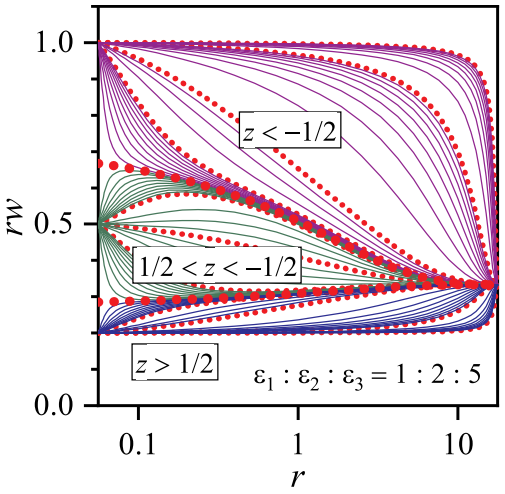

Fig. 2. Dependences $rw(r)$ for two point charges equivalently located ($z_1 = z_2 = z$) in a three-layer structure with the layer dielectric constants $\{\varepsilon_i\} = 1:2:5$ at various z's from $z = -100$ (top) to $z = 100$ (bottom). Here, r and z are dimensionless (normalized by the slab width L) charge coordinates R and Z, respectively (see Fig. 1), and w is the normalized Coulomb interaction energy between the charges. Bold dotted curves correspond to the interfaces $z = \pm\frac{1}{2}$. Thin dotted curves correspond to $z = 0, \pm 0.4, \pm 0.6, \pm 1, \pm 10, \pm 100$. Solid curves correspond to various z's varying with steps of 0.1 in the interval $|z| < 1$, 1 in the intervals $1 < |z| < 10$, and 10 in the intervals $10 < |z| < 100$. In the intervals $0.4 < |z| < 0.6$, z is varied with a step of 0.01 in order to illustrate the transformation of curves when crossing the interfaces. See further explanations in the text.

out of the question. Nevertheless, attention should be paid to some points.

At the right axis ($r \to \infty$), all plots form a single node corresponding to the long-range Coulombic asymptotics with coefficient (15); this is case (iv) in section 2.2. At the left axis ($r \to 0$), we can distinguish five nodes corresponding to the short-range Coulombic asymptotics with coefficients (16); this is case (i) for the charges in the medium bulk and case (ii) for the charges located at either of the interfaces. Finally, the flattening of the curves corresponding to large z amplitudes at the same rw values (those values equal ε_1^{-1} for $z < 0$ and ε_3^{-1} for $z > 0$) illustrates the case (iii). Thus, a partial answer to question (A) in section 2.2 at the qualitative level is as follows: Since every curve in Fig. 2 continuously tends from one of the nodes at the left ordinate axis to the common node at the right ordinate axis, the non-constant value of the product rw is guaranteed, which means that the dependence $w(r)$ is non-Coulombic. Now, let us made further, more quantitative, estimations.

The dependences $N(r)$ calculated for various $w(r, z = \text{var})$ profiles in the case of the same toy structure with $\{\varepsilon_i\} = 1 : 2 : 5$ are presented in Fig. 3. The calculation was carried out following the procedure described in section 2.3. The non-constancy of $N(r)$ is evident. The specific forms of those curves are determined by the parameters z and $\{\varepsilon_i\}$ and can be rather intricate. Both underscreening ($N > -1$) and overscreening ($N < -1$) of interaction between the charges can take place. We think that the exhibited deviations from the clasical value $N = -1$ cannot be characterized as weak, moderate, or strong, because such an estimate should be based on the profile $w(r)$ itself. Nevertheless, the $N(r)$ dependence may be important, e.g., while considering the formation of surface patterns displayed by charges adsorbed on a pristine or a film-coated surface. Indeed, in this case a subtle interplay of parameters determines possible adsorbate structures and phase transitions between them [65,66].

In Figs. 4 and 5, analogous $N(r)$ dependences are depicted for three-layer structures with $\{\varepsilon_i\} = 2 : 1 : 5$ and $1 : 5 : 2$, i.e. qualitatively different permutations of the dielectric constants. The general qualitative picture remains the same.

Now, we have a good opportunity to complete our previous answer to question (A) and illustrate why the Coulombic-like dependence (1) should be applied carefully when describing interaction between two point charges near a medium interface. We will also analyze the quality of the proposed interpolation formula (18), in which the value of N is determined from the local behavior of the dependence $w(r)$.

Fig. 6 (the upper panel) demonstrates the rw profile (the dotted curve) for the problem parameters $\{\varepsilon_i\} = 1 : 2 : 5$ (see Fig. 2) and $z = -0.55$. Bright circles mark a set of examined intervals between the

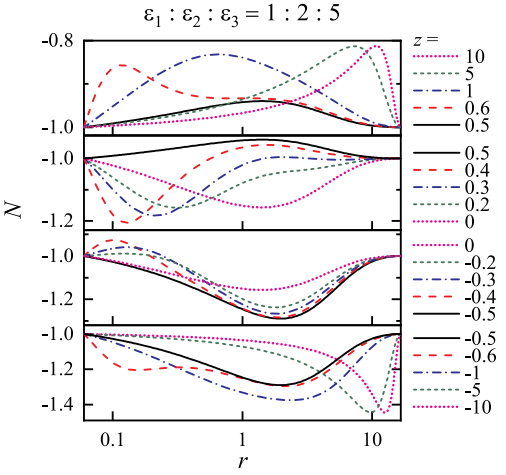

Fig. 3. Dependences of the effective power exponent N in formula (18) on r for various charge coordinates $z_1 = z_2 = z$ in the three-layer structure with the layer dielectric constants $\{\varepsilon_i\} = 1 : 2 : 5$. See further explanations in the text.

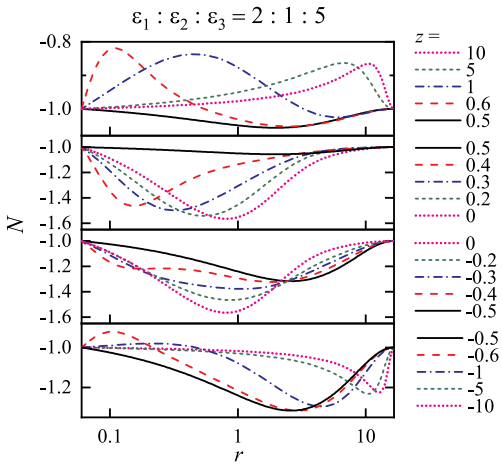

Fig. 4. The same as in Fig. 3, but for the three-layer structure with $\{\varepsilon_i\} = 2 : 1 : 5$.

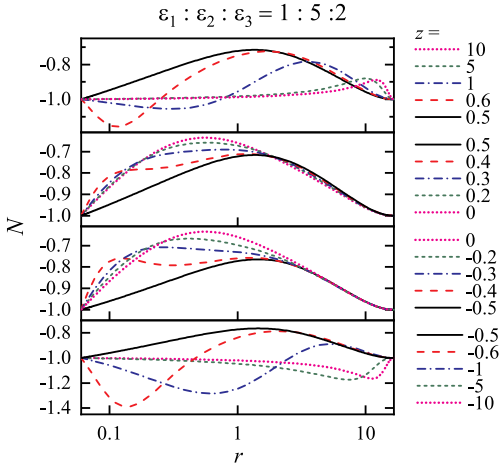

Fig. 5. The same as in Fig. 3, but for the three-layer structure with $\{\varepsilon_i\} = 1 : 5 : 2$.

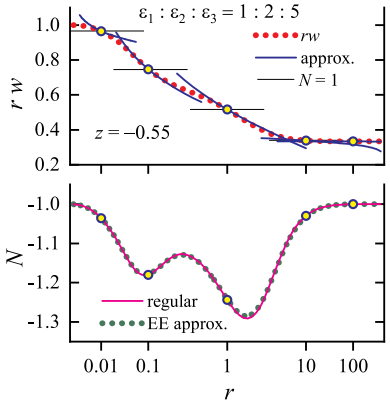

Fig. 6. (Upper panel) The rw profile (the dotted curve) and its approximations (solid curves) for two point charges with $z_1 = z_2 = z = -0.55$ in the three-layer structure with $\{\varepsilon_i\} = 1 : 2 : 5$. (Lower panel) The corresponding $N(r)$ dependences obtained by regular numerical calculations (the solid curve) and in the framework of the effective exponential (EE) approximation (the dotted curve). See further explanations in the text.

charges ($r = 0.01, 0.1, 1, 10, 100$). If the interaction between those charges were pure Coulombic ($N = -1$) in the vicinity of any examined point, we would have obtained a horizontal line for the $rw(r)$ dependence within this vicinity (thin lines). Obviously, this is not the case except for sufficiently short [case (i)] and sufficiently long [case (iv)] r values. The dependence $N(r)$ for the apparent N value calculated by formula (21) is shown in the lower panel. One can see that the true Coulombic regime ($N = -1$) takes place only in the limiting cases $r \to 0$ and $r \to \infty$. From Figs. 3–5, it is also evident that the parameter N can become equal to -1 at finite r's only occasionally, when passing from $N > -1$ to $N < -1$ or vice versa.

The approximation of the rw-dependence at each examined point with the help of Eq. (18), in which the value of the "constant" multiplier $C(r_0)$ was determined making use of the corresponding w- and N-values, is depicted in the upper panel by solid segments. Attention should be drawn to the fact that the intervals of approximation validity turned out rather wide. In particular, in the case $r_0 = 1$, formula (18) with the relevant (calculated at $r_0 = 1$) values of the parameters $C(r_0)$ and $N(r_0)$ provides the description of the actual $w(r)$ dependence with a relative accuracy not worse that 10% within an interval $0.3 \lesssim r \lesssim 8.5$.

Thus, the application of formula (18) is justified, but the calculation procedure for N on the basis of regular method is rather cumbersome. In [36], we proposed the so-called "effective-exponential" (EE) approximation for the $w(r)$ dependence. More specifically, it results in a finite sum (about a dozen of summands) of terms like Eq. (20). At comparable ε_i values, this approximation provides a very high accuracy within the whole r-interval, $0 \le r < \infty$ (for more details, see [36]). In particular, the approximation for the $w(r)$ dependence shown in Fig. 2(a) equals (all coefficients are rounded to three digits after the decimal point)

$$w(r) \approx \frac{1}{r} - \frac{0.333}{\sqrt{r^2 + 0.010}} - \frac{0.125}{\sqrt{r^2 + 3.505}} + \frac{0.042}{\sqrt{r^2 + 3.890}} + \frac{0.143}{\sqrt{r^2 + 4}} - \frac{0.429}{\sqrt{r^2 + 4.410}} - \frac{0.018}{\sqrt{r^2 + 14.994}} + \frac{0.054}{\sqrt{r^2 + 15.779}}.$$

The application of formula (21) gives the $N(r)$ dependences shown in the lower panel of Fig. 6 by the solid (the result of the regular numerical calculation) and dotted (the EE approximation) curves.

3.2. Symmetric structures

To shorten the number of problem parameters, let us consider the case of symmetric structures with $\varepsilon_1 = \varepsilon_3 \neq \varepsilon_2$.

In our previous publication [34], we showed that, in the two-layer system, the deviation from the pure Coulombic behavior is stronger if either $\varepsilon_1 \gg \varepsilon_2$ or vice versa. The theoretical limit is achieved when two charges are located, e.g., in medium 1 with the dielectric permittivity ε_1 and near the surface of medium 2 with the dielectric permittivity $\varepsilon_2 \to \infty$ (the ideal conductor of the classical electrostatics [31,32]). Due to the interference of image charge electric fields, in this limiting case one obtains the interaction between two point-like dipoles described by the power exponent $N = -3$.

Therefore, our calculations for the three-layer systems were also carried out for some ε_i-combinations with sufficiently high ratios between the dielectric permittivities of the slab and covers; namely, 10:1 and 1:10 (Fig. 7), and 100:1 and 1:100 (Fig. 8). One can see that, with the increase of this permittivity, the maximum deviations from the value $N = -1$ toward under- and overscreening become larger.

Let us first examine structures with the interlayer having a large ε_2 and suspended in the vacuum, i.e. $\varepsilon_1 = \varepsilon_3 = 1$ (panels (a) in Figs. 7 and 8). The dash-dot-dot curves in those panels correspond to two charges located in the vacuum in a close vicinity of the interface with the large-ε medium (for instance, a ferroelectric film). At small r, the curves possess an acute and deep minimum, which approaches a value of -3 at $\varepsilon_2 \to \infty$

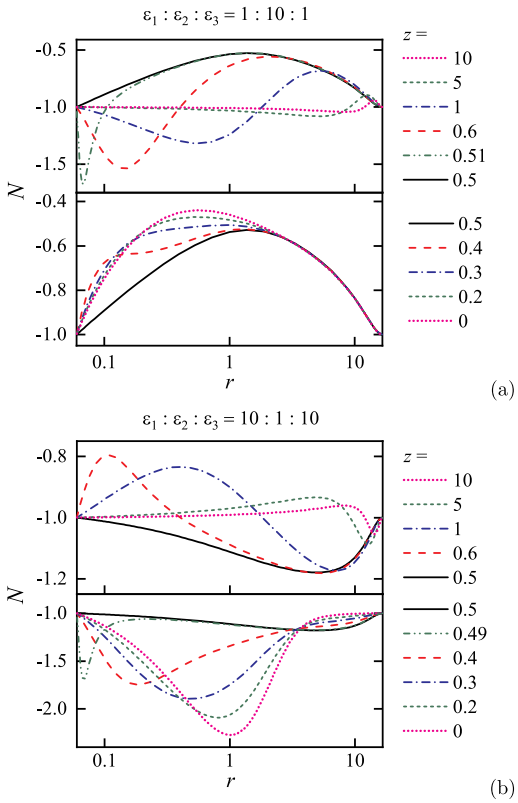

Fig. 7. The same as in Fig. 3, but for the symmetric three-layer structures with $\{\varepsilon_i\} = 1 : 10 : 1$ (panel a) and $\{\varepsilon_i\} = 10 : 1 : 10$ (panel b).

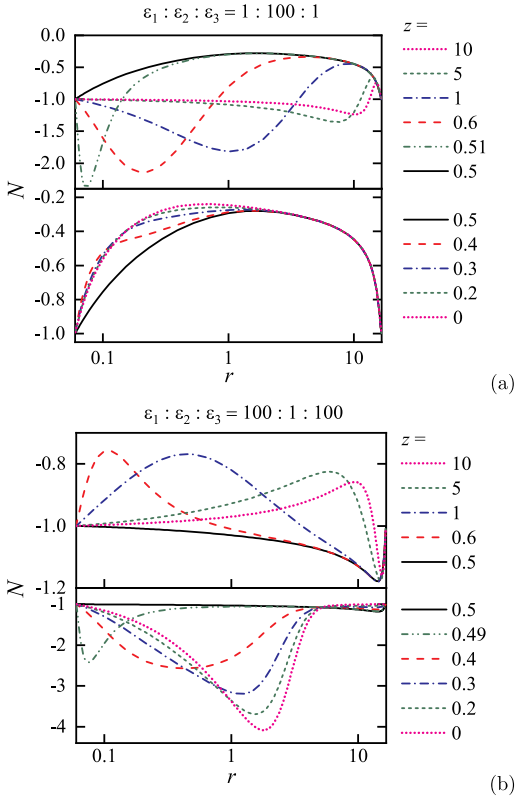

Fig. 8. The same as in Fig. 3, but for the symmetric three-layer structures with $\{\varepsilon_i\} = 1 : 100 : 1$ (panel a) and $\{\varepsilon_i\} = 100 : 1 : 100$ (panel b).

and $r \to 0$. This is an analog of the dipole-dipole interaction in the two-layer system that was mentioned above and studied previously [34]. A comparison of the results obtained for two-layer and three-layer configurations makes it evident that the influence of the second interface significantly affects the behavior of the dependences $w(r,z)$.

At the same time, Figs. 7(b) and 8(b) demonstrate a rather unexpected result. Namely, the overscreening ($N < -1$) of the charge located in the middle of the vacuum gap between two ferroelectric, semimetallic or metallic covers can be stronger than that near the cover surface. It means that, in this respect, the polarization charges at the both interfaces act synergistically. The corresponding N minimum becomes deeper and shifts toward larger r's as the dielectric permittivity of covers grows. In particular, in Fig. 8(a), it has already exceeded a value of -3 discussed above. In this connection, there arises a question: Is there a theoretical lower limit for the N value in the three-layer geometry and, if any, where is this minimum located? To answer it, we should calculate w in the limit $\varepsilon_1 : \varepsilon_2 : \varepsilon_3 = \infty : 1 : \infty$, starting from formula (21). After some algebra using Eqs. (7–17) with $\varepsilon_1 = \varepsilon_3 = \infty$ and $\varepsilon_2 = 1$, we obtain the equation

$$w(r, z_1 = z_2 = 0) = \int_0^\infty dq\, J_0(rq) \tanh\left(\frac{q}{2}\right). \tag{22}$$

Let us find its short- and long-range asymptotics. Taking into account that, by changing the integration variable $rq \to x$, the previous formula is transformed to the expression

$$w(r) = \frac{1}{r}\int_0^\infty dx\, J_0(x) \tanh\left(\frac{x}{2r}\right) \tag{23}$$

and passing to the limit $r \to 0$ in the integrand, we arrive at the short-range asymptotics

$$w(r \ll 1, z_1 = z_2 = 0) \approx \frac{1}{r}. \tag{24}$$

It is of no wonder, since if the charges concerned are located extremely close to each other at the center of the vacuum gap they do not "feel" the interfaces.

In the long-range case, it is worthwhile to use the expansion [67].

$$\tanh\frac{\pi x}{2} = \frac{4x}{\pi}\sum_{k=1}^{\infty}\frac{1}{(2k-1)^2 + x^2} \tag{25}$$

and the tabulated integral

$$\int_0^\infty dx\, J_0(ax)\frac{x}{b^2 + x^2} = K_0(ab) \tag{26}$$

where K_0 is the modified Bessel function of the second kind. Then, we arrive at the expression

$$w(r, z_1 = z_2 = 0) = 4\sum_{k=1}^{\infty} K_0[(2k-1)\pi r]. \tag{27}$$

The summands in this series decrease exponentially as k grows. Therefore, since at $x \gg 1$,

$$K_0(x \gg 1) \approx \left(\frac{\pi}{2x}\right)^{1/2} \exp(-x)\left(1 - \frac{1}{8x}\right),$$

the long-range asymptotics reads

$$w(r \gg 1, z_1 = z_2 = 0) \approx \left(\frac{8}{r}\right)^{1/2} \exp(-\pi r). \tag{28}$$

An attempt to obtain a power-law asymptotics $w(r \gg 1) \approx Cr^N$ for this expression brings about $N \to -\infty$. This result can be easily interpreted: if two charges are in a narrow gap between two covers, then this gap effectively disappears in the limiting case $r \to \infty$, and the charges become embedded into an ideal conductor continuum with $\varepsilon \to \infty$, so that their interaction is completely screened out.

The calculation of the $w(z = 0, r)$ dependence at $\varepsilon_1 : \varepsilon_2 : \varepsilon_3 = \infty : 1 : \infty$ for intermediate r's was carried out using formulas (21) and (27). The result is shown in Fig. 9 by the dotted curve, and it confirms the both asymptotics (24) and (28). But it does not obey relation $rw \to 2/(\varepsilon_1 + \varepsilon_3)$, which is mandatory for any finite dielectric permittivity values of the covers. In the latter case, $N(r \to \infty) \to -1$. How can those two different limits be put in agreement with each other? Fig. 9 also gives an answer to this question: as the cover dielectric constant $\varepsilon_1 = \varepsilon_3 \equiv \varepsilon$ tends to ∞, the $w(r)$ profiles (solid curves) evolve to the limiting case (dotted curve). It is worth indicating that the N minimum deepens and shifts towards larger r's very slowly, and $N(r \to \infty) \to -1$ for any finite ε. Hence, the case $\varepsilon_1 : \varepsilon_2 : \varepsilon_3 = \infty : 1 : \infty$ is a true singular limit, and the corresponding $w(r)$ profiles converge to this limit nonuniformly at $r \to \infty$.

3.3. Example

It stems from the results of our calculations and the corresponding discussion that the intrinsic dielectric inhomogeneity of layered heterostructures severely distorts the parent Coulomb interaction between two point charges immersed into either of three media. The apparent non-Coulombic behavior may influence a lot of conclusions concerning charge-charge interaction in layered structures important for electronics and biophysics, which were made without any reference to this basic fact. Although our approach to the problem is quite transparent and relatively well known, the inevitable and conspicuous violation of the Coulomb law in such a situation was not adequately emphasized both in the original papers and textbooks.

As a practically important example, let us consider the interaction of two electrons suspended above the surface of a liquid helium film (medium 2). The latter is located above a metal or semiconductor electrode (medium 1) [12–15,26,68].

The measured dielectric constant of liquid $_4$He is about 1.06 [69,70], and this value was used in calculations ($\varepsilon_2 = 1.06$). Medium 3, in which the electrons "hover" over the free helium surface is helium vapor, air, or vacuum. In each case, the corresponding dielectric permittivity is close or strictly equal to unity ($\varepsilon_3 = 1$). For the substrate (medium 1), we selected two typical cases. It was either a semiconductor with $\varepsilon_1 = 10$ or a metal modelled as a medium with $\varepsilon_1 = 1000$. For both substrates, the difference between ε_2 and ε_3 is much smaller that the difference between either of those quantities and ε_1. Moreover, the actual distances of the suspended electrons from the cryogenic liquid surfaces are indeed small enough (the quantum-mechanical average distance from the substrate of the electron in the ground state is about 100 Å). Therefore, it is sufficient to consider one charge configuration with the z-coordinate of both electrons equal to $\frac{1}{2}$. In other words, they almost "lie" on the free helium surface. Fig. 10 demonstrates the corresponding $rw(r)$ and $N(r)$ dependences. Again, one can see how the standard Coulomb behavior is restored at $r \to 0$ and $r \to \infty$. When the substrate is a metal, the interaction becomes a dipole-dipole-like one, as can be easily shown analytically

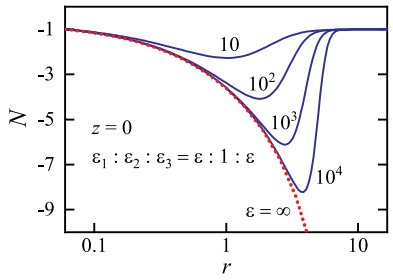

Fig. 9. The $N(r)$ dependences for two point charges located in the central plane of the slab ($z = 0$) in the case of the symmetric three-layer structures, $\{\varepsilon_i\} = \varepsilon : 1 : \varepsilon$, with various ε's (solid curves). The dotted curve corresponds to the limit $\varepsilon \to \infty$.

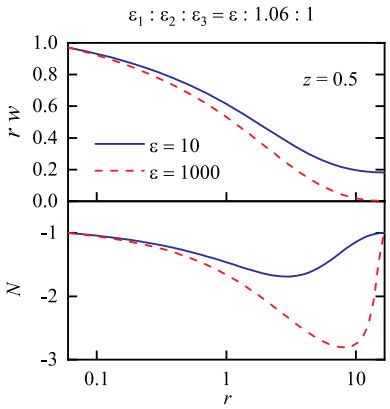

Fig. 10. (Upper panel) The *rw* profiles for electrons suspended above ($z = \frac{1}{2}$) liquid helium films covering substrates with various dielectric permittivities ε's [the three-layer structures with $\{\varepsilon_i\} = \varepsilon : \varepsilon_{He^4}(\approx 1.06) : 1$]. (Lower panel) The corresponding $N(r)$ dependences obtained by regular numerical calculations. See further explanations in the text.

[12]. But a discussed value of −3 is not achieved because of the "finite" ε_1 and the availability of the liquid helium film. On the other hand, if the substrate is a "standard" insulator, its influence is much weaker. It is of no wonder, because in this case the whole structure is dielectrically more homogeneous. Nevertheless, the naively expected parent Coulombic behavior of the interaction between the charges is reproduced nowhere.

4. The case $\left(z_1 = -\frac{1}{2}, z_2 = \frac{1}{2}\right)$. Electrostatic interaction across the interlayer

The analysis of the Coulomb law violations in the case when charges are located at different interfaces is no less important for many fundamental and practical problems. In particular, the interaction of charges through a slab is of special interest for the problems of exciton spectra in heterostructures [9,37,40–43,71] or monolayers [44–46], as well as those concerning exciton (electron-hole) superfluidity in layered systems [47,49,50,52–55] and related topics [41,72–75]. Sometimes, the actual electron-electron or electron-hole interaction is regarded to be a conventional Coulombic repulsion and attraction, respectively, whatever the relationship between the dielectric constants of the constituent media. However, the Coulombic character of the electrostatic interaction must be proved or refuted in this case similarly as has been made above for the configuration $z_1 = z_2$. It is remarkable that a popular and often successful Rytova-Keldysh approximation [37,76] to the electrostatic interaction in the configuration concerned ($z_1 = -\frac{1}{2}, z_2 = \frac{1}{2}$) is far from being Coulomb-like, which is not surprising.

For this charge configuration, the normalized distance between the charges equals

$$s = \sqrt{r^2 + 1}. \tag{29}$$

On the other hand, the lateral distance *r* is more interesting from the experimental viewpoint, in particular, when studying a possibility and features of the excitonic superfluidity [47–50]. Therefore, in order to analyze the violations of the Coulomb law, we use *r* as the variable of the interaction energy $w(r)$. As a result, formula (19) now reads

$$N = \frac{r^2 + 1}{r} \frac{d}{dr} \ln w. \tag{30}$$

Fig. 11 demonstrates the effective underscreening of the electrostatic interaction across the slab in the symmetric three-layer heterostructures. As might be expected, the deviations from the conventional Coulomb behavior are especially conspicuous if the dielectric constants in the covers and the interlayer differ substantially.

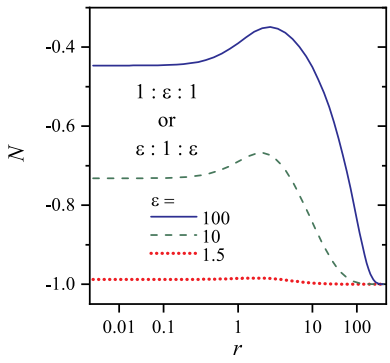

Fig. 11. The $N(r)$ dependences for two point charges located at different interfaces ($z_1 = -\frac{1}{2}, z_2 = \frac{1}{2}$) of the symmetric three-layer structures. See further explanations in the text.

At the same time, it can be shown that an interesting symmetry relation takes place for the interaction between two point charges located in different cover layers of the studied heterostructure:

$$\frac{w\left(z_1 \le -\frac{1}{2}, z_2 \ge \frac{1}{2}, r; \varepsilon_1 = \varepsilon_3 = \varepsilon', \varepsilon_2 = \varepsilon''\right)}{w\left(z_1 \le -\frac{1}{2}, z_2 \ge \frac{1}{2}, r; \varepsilon_1 = \varepsilon_3 = \varepsilon'', \varepsilon_2 = \varepsilon'\right)} = \frac{\varepsilon''}{\varepsilon'}. \tag{31}$$

This relation is valid in the limiting case $\left(z_1 = -\frac{1}{2}, z_2 = \frac{1}{2}\right)$ as well. Therefore, a plot of the dependence $sw(s)$ for the dielectric set $\{\varepsilon_i\} = a : b : a$ can be obtained from the plot for the dielectric set $\{\varepsilon_i\} = b : a : b$ by simply changing the Y-axis scale by the corresponding factor. However, this factor drops out after the derivative is taken in Eq. (30). As a result, the plots $N(s)$ [or $N(r)$] are absolutely identical for both those sets.

Our calculations clearly demonstrate that the Coulomb law is never fulfilled for charge-charge interaction across the slab. However, it is approximately valid when the ratio $\varepsilon''/\varepsilon'$ is close to unity. This situation is realized in many heterostructures, e.g., constructed of doped III-V semiconductor alternating layers [3,77]. In the opposite case, e.g., when the researchers are dealing with ferroelectric films surrounded by traditional semiconductors or are suspended in the vacuum (such a configuration was considered by Keldysh [37]), Coulomb law is considerably distorted (see Fig. 11).

It seems instructive to analyze the correlation of the curves $N(s)$ displayed in Fig. 11 with the normalized dependences *sw*, similarly to

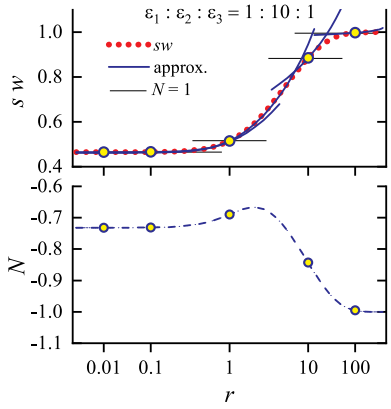

Fig. 12. (Upper panel) The *sw* profile (the dotted curve) and its approximations (solid curves) for two point charges located at different interfaces ($z_1 = -\frac{1}{2}$, $z_2 = \frac{1}{2}$) of the symmetric three-layer structure with $\{\varepsilon_i\} = 1 : 10 : 1$. (Lower panel) The corresponding $N(r)$ dependence obtained by regular numerical calculations. See further explanations in the text.

what was done in Section 3 for the case of equivalently located charges ($z_1 = z_2$, see Fig. 6). Such a comparison is demonstrated in Fig. 12 for a specific configuration $\{\varepsilon_i\} = 1 : 10 : 1$. One sees that the approximation of the effective power exponent, $N(s) \approx N(s_0)$, works well in wide intervals around different points s_0, whereas the naive Coulomb dependence with $N = 1$ fails everywhere except in the asymptotic region $r \to \infty$.

5. Conclusions

We analyzed the charge-charge electrostatic interaction $W_{Q_1Q_2}$ in three-layer planar structures. The dielectric functions of the media were considered as classical constants. Two particular charge configurations were analyzed in more detail. Those are the cases when Z-coordinates of the charges, perpendicular to the interfaces, are identical ($Z_1 = Z_2$) and when the charges are located across the interlayer. It was shown that the textbook Coulomb charge-charge interaction $W_{Q_1Q_2} \sim S^{-1}$, where S is the distance between the charges, is violated due to the complex character of the screening and the appearance of polarization charges at the both interfaces. It means that the problem is essentially a many-body one. It was demonstrated that both underscreening and overscreening of the electrostatic interaction may happen depending on the ratios between the dielectric constants of constituent layers. The approximation proposed by the authors allows to analytically treat the cumbersome problem and obtain working formulas to be used as inputs to solve many specific issues in physics of layered structures. For instance, those formulas can be used in the calculations of the exciton spectra in three-layered structures as well as in two-dimensional crystals (monolayers). The problem of the exotic but highly expected electron-hole superfluidity based on the Coulomb interaction also depends on the proper treatment of the electrostatic phenomena in three-layer structures.

Declaration of competing interest

There is no conflict of interest among the authors.

Acknowledgements

The work was partially supported by the Project N 22 of the 2018–2020 Scientific Cooperation Agreement between Poland and Ukraine. The research was also partially supported by the NAS of Ukraine (Grant Nos. 1.4.B-179, VC-188, and VC-202) and the Polish NCN grant 2015/19/B/ST4/02721.

References

[1] L.V. Keldysh, Excitons and polaritons in semiconductor/insulator quantum wells and superlattices, Superlattice Microstruct. 4 (1988) 637–642, https://doi.org/10.1016/0749-6036(88)90253-4.
[2] E.P. Pokatilov, S.I. Beril, V.M. Fomin, V.V. Kalinovskii, The size-quantized states of the Wannier-Mott exciton in structures with superthin films of CdTe, Phys. Status Solidi B 161 (1990) 603–612, https://doi.org/10.1002/pssb.2221610215.
[3] F.T. Vasko, A.V. Kuznetsov, Electronic States and Optical Transitions in Semiconductor Heterostructures, Springer Verlag, New York, 1999.
[4] S.B. Ogale, Thin Films and Heterostructures for Oxide Electronics, Springer Verlag, New York, 2010.
[5] C. Lamberti, G. Agostini (Eds.), Characterization of Semiconductor Heterostructures and Nanostructures, second ed., Elsevier, Oxford, 2013.
[6] A.K. Geim, I.V. Grigorieva, Van der Waals heterostructures, Nature 499 (2013) 419–425, https://doi.org/10.1038/nature12385.
[7] K.S. Novoselov, A. Mishchenko, A. Carvalho, A.H. Castro Neto, 2D materials and van der Waals heterostructures, Science 353 (2016) aac9439, https://doi.org/10.1126/science.aac9439.
[8] D. Jariwala, T.J. Marks, M.C. Hersam, Mixed-dimensional van der Waals heterostructures, Nat. Mater. 16 (2017) 170–181, https://doi.org/10.1038/NMAT4703.
[9] T.C. Berkelbach, D.R. Reichman, Optical and excitonic properties of atomically thin transition-metal dichalcogenides, Annu. Rev. Condens. Matter Phys. 9 (2018) 379–396, https://doi.org/10.1146/annurev-conmatphys-033117-054009.
[10] J.P. Colinge, C.A. Colinge, Physics of Semiconductor Devices, Kluwer Academic, New York, 2002.
[11] Y. Fu, Physical Models of Semiconductor Quantum Devices, Springer Verlag, Dordrecht, 2014.
[12] V.B. Shikin, Yu P. Monarkha, Two-Dimensional Charged Systems in Helium, Nauka, Moscow, 1989 in Russian.
[13] E.Y. Andrei (Ed.), Two-Dimensional Electron Systems on Helium and Other Cryogenic Substrates, Kluwer Academic, Dordrecht, 1997.
[14] Y. Monarkha, K. Kono, Two-Dimensional Coulomb Liquids and Solids, Springer Verlag, New York, 2004.
[15] E.S. Sokolova, S.S. Sokolov, Energy spectrum of surface electrons over the ^{3}He-^{4}He solution film with inhomogeneous isotope distribution, Fiz. Nizk. Temp. 45 (2019) 46–57 [doi 10.1063/1.5082309] [Low Temp. Phys. 45 (2019) 39–48].
[16] Yu A. Romanov, Theory of characteristic energy losses in thin films, Zh. Eksp. Teor. Fiz. 47 (1964) 2119–2133 [Sov. Phys. JETP 20 (1965) 1424–1432].
[17] A.M. Gabovich, E.A. Pashitskii, S.K. Uvarova, Plasmon and exciton superconductivity mechanism in layered structures, Fiz. Nizk. Temp. 1 (1975) 984–995.
[18] A.A. Kornyshev, A.I. Rubinshtein, M.A. Vorotyntsev, Image potential near a dielectric-plasma-like medium interface, Phys. Status Solidi B 84 (1977) 125–132, https://doi.org/10.1002/pssb.2220840114.
[19] A.M. Gabovich, L.G. Il'chenko, E.A. Pashitskii, Electrostatic charge interaction with surfaces of metals and semiconductors, Fiz. Tverd. Tela 21 (1979) 1683–1689 [Sov. Phys. Solid State 21 (1979) 965–969].
[20] A.M. Gabovich, L.G. Il'chenko, E.A. Pashitskii, Yu A. Romanov, Electrostatic energy and screened charge interaction near the surface of metals with different Fermi surface shape, Surf. Sci. 94 (1980) 179–203, https://doi.org/10.1016/0039-6028(80)90163-6.
[21] L.G. Il'chenko, E.A. Pashitskii, Yu A. Romanov, Electrostatic charge potential in layered systems with spatial dispersion, Fiz. Tverd. Tela 22 (1980) 2700–2710.
[22] L.G. Il'chenko, E.A. Pashitskii, Yu A. Romanov, Charge interaction in layered systems, Fiz. Tverd. Tela 22 (1980) 3395–3401.
[23] A.M. Gabovich, L.G. Il'chenko, E.A. Pashitskii, Energy spectrum of electrons above a thin liquid helium film in a clamping electrical field, Zh. Eksp. Teor. Fiz. 81 (1981) 2063–2069 [Sov. Phys. JETP 54 (1981) 1089–1092].
[24] A.A. Kornyshev, M.A. Vorotyntsev, J. Ulstrup, The effect of spatial dispersion of the dielectric permittivity on the capacitance of thin insulating films: non-linear dependence of the inverse capacitance on film thickness, Thin Solid Films 75 (1981) 105–118, https://doi.org/10.1016/0040-6090(81)90445-4.
[25] L.G. Il'chenko, E.A. Pashitskii, Yu A. Romanov, Charge interaction in layered systems with spatial dispersion, Surf. Sci. 121 (1982) 375–395, https://doi.org/10.1016/0039-6028(82)90249-7.
[26] A.M. Gabovich, L.G. Il'chenko, E.A. Pashitskii, Image force and electron spectrum at the surface of liquid helium, Surf. Sci. 130 (1983) 373–394, https://doi.org/10.1016/0039-6028(83)90368-0.
[27] F. Bechstedt, R. Enderlein, Dielectric screening, polar phonons, and longitudinal electronic excitations of quantum well double heterostructures. Application to light scattering from charge density fluctuations, Phys. Status Solidi B 131 (1985) 53–66, https://doi.org/10.1002/pssb.2221310104.
[28] A.M. Gabovich, V.M. Rosenbaum, A.I. Voitenko, Dynamical image forces in three-layer systems and field emission, Surf. Sci. 186 (1987) 523–549, https://doi.org/10.1016/S0039-6028(87)80392-8.
[29] E.P. Pokatilov, V.M. Fomin, S.I. Beril, Oscillatory Excitations, Polarons and Excitons in Multilayer Systems and Superlattices, Shtiintsa, Kishinev, 1990 in Russian.
[30] W. Thomson, in: W. Thomson (Ed.), In: the Cambridge and Dublin Mathematical Journal, vol. III, Macmillan, Barclay, and Macmillan, Cambridge, 1848.
[31] W.R. Smythe, Static and Dynamic Electricity, McGraw-Hill, New York, 1950.
[32] J.D. Jackson, Classical Electrodynamics, John Wiley and Sons, New York, 1998.
[33] I.E. Tamm, Foundations of Electricity Theory, Nauka, Moscow, 1976 in Russian.
[34] A.M. Gabovich, A.I. Voitenko, The 'non-Coulombic' character of classical electrostatic interaction between charges near interfaces, Eur. J. Phys. 39 (2018) 45203, https://doi.org/10.1088/1361-6404/aabbf9.
[35] A.M. Gabovich, L.G. Il'chenko, E.A. Pashitskii, Yu A. Romanov, Charge screening and electron density Friedel oscillations in metals with different Fermi surface shape, Zh. Eksp. Teor. Fiz. 75 (1978) 249–264 [Sov. Phys. JETP 48 (1978) 124–131].
[36] A.M. Gabovich, A.I. Voitenko, Electrostatic interaction of point charges in three-layer structures: the classical model, Condens. Matter 4 (2019) 44, https://doi.org/10.3390/condmat4020044.
[37] L.V. Keldysh, Coulomb interaction in thin semiconductor and semimetal films, Pis'ma Zh. Eksp. Teor. Fiz. 29 (1979) 716–719 [JETP Lett. 29 (1979) 658–661].
[38] V.M. Fomin, E.P. Pokatilov, Excitons in multi-layer systems, Phys. Status Solidi B 129 (1985) 203–209, https://doi.org/10.1002/pssb.2221290120.
[39] E.P. Pokatilov, S.I. Beril, V.M. Fomin, G.A. Pogorilko, Wannier-Mott exciton states in two-layer periodic structures, Phys. Status Solidi B 130 (1985) 619–628, https://doi.org/10.1002/pssb.2221300225.
[40] M.N. Brunetti, O.L. Berman, R.Ya Kezerashvili, Optical properties of excitons in buckled two-dimensional materials in an external electric field, Phys. Rev. B 98 (2018) 125406, https://doi.org/10.1103/PhysRevB.98.125406.
[41] G. Wang, A. Chernikov, M.M. Glazov, T.F. Heinz, X. Marie, T. Amand, B. Urbaszek, Colloquium: excitons in atomically thin transition metal dichalcogenides, Rev. Mod. Phys. 90 (2018) 21001, https://doi.org/10.1103/RevModPhys.90.021001.
[42] N.A. Asriyan, I.L. Kurbakov, A.K. Fedorov, Y.E. Lozovik, Optical probing in a bilayer dark-bright condensate system, Phys. Rev. B 99 (2019) 85108, https://doi.org/10.1103/PhysRevB.99.085108.

[43] J.-Z. Zhang, J.-Z. Ma, Two-dimensional excitons in monolayer transition metal dichalcogenides from radial equation and variational calculations, J. Phys. Condens. Matter 31 (2019) 105702, https://doi.org/10.1088/1361-648X/aaf8c5.
[44] E. Liu, J. van Baren, T. Taniguchi, K. Watanabe, Y.-C. Chang, C.H. Lui, Magnetophotoluminescence of exciton Rydberg states in monolayer WSe_2, Phys. Rev. B 99 (2019) 205420, https://doi.org/10.1103/PhysRevB.99.205420.
[45] C. Katan, N. Mercier, J. Even, Quantum and dielectric confinement effects in lower-dimensional hybrid perovskite semiconductors, Chem. Rev. 119 (2019) 3140–3192, https://doi.org/10.1021/acs.chemrev.8b00417.
[46] B. Scharf, D.V. Tuan, I. Žutić, H. Dery, Dynamical screening in monolayer transition-metal dichalcogenides and its manifestations in the exciton spectrum, J. Phys. Condens. Matter 31 (2019) 203001, https://doi.org/10.1088/1361-648X/ab071f.
[47] Yu E. Lozovik, V.I. Yudson, Feasibility of superfluidity of paired spatially-separated paired electrons and holes; a new superconductivity mechanism, Pis'ma Zh. Eksp. Teor. Fiz. 22 (1975) 556–559 [JETP Lett. 22 (1975) 274–276].
[48] Yu E. Lozovik, V.I. Yudson, A new mechanism for superconductivity: pairing between spatially separated electrons and holes, Zh. Eksp. Teor. Fiz. 71 (1976) 738–753 [Sov. Phys. JETP 44 (1976) 389–397].
[49] I.O. Kulik, S.I. Shevchenko, Excitonic pairing and superconductivity in layered systems, Fiz. Nizk. Temp. 2 (1976) 1405–1426.
[50] S.I. Shevchenko, I.O. Kulik, Electrodynamics of exciton pairing in low-dimensionality crystals without inversion centers, Pis'ma Zh. Eksp. Teor. Fiz. 23 (1976) 171–173 [JETP Lett. 23 (1976) 150–152].
[51] S.I. Shevchenko, Theory of superconductivity for systems with pairing of spatially-separated electrons and holes, Fiz. Nizk. Temp. 2 (1976) 505–516.
[52] D.V. Fil, S.I. Shevchenko, Electron-hole superconductivity (Review Article), Fiz. Nizk. Temp. 44 (2018) 1111–1160 [Low Temp. Phys. 44 (2018) 867–909].
[53] O.L. Berman, R.Y. Kezerashvili, Superfluidity of dipolar excitons in a transition metal dichalcogenide double layer, Phys. Rev. B 96 (2017) 94502, https://doi.org/10.1103/PhysRevB.96.094502.
[54] S. Saberi-Pouya, M. Zarenia, A. Perali, T. Vazifehshenas, F.M. Peeters, High-temperature electron-hole superfluidity with strong anisotropic gaps in double phosphorene monolayers, Phys. Rev. B 97 (2018) 174503, https://doi.org/10.1103/PhysRevB.97.174503.
[55] S. Conti, A. Perali, F.M. Peeters, D. Neilson, Multicomponent screening and superfluidity in gapped electron-hole double bilayer graphene with realistic bands, Phys. Rev. B 99 (2019) 144517, https://doi.org/10.1103/PhysRevB.99.144517.
[56] A.V. Sidyakin, Calculation of the polarization contribution to the energy of interaction of a charge with the surface of a metal, Zh. Eksp. Teor. Fiz. 58 (1970) 573–581 [Sov. Phys. JETP 31 (1970) 308–312].
[57] D.E. Beck, V. Celli, Linear response of a metal to an external charge distribution, Phys. Rev. B 2 (1970) 2955–2960, https://doi.org/10.1103/PhysRevB.2.2955.
[58] D.M. Newns, Dielectric response of a semi-infinite degenerate electron gas, Phys. Rev. B 1 (1970) 3304–3322, https://doi.org/10.1103/PhysRevB.1.3304.
[59] J. Heinrichs, Response of metal surfaces to static and moving point charges and to polarizable charge distributions, Phys. Rev. B 8 (1973) 1346–1364, https://doi.org/10.1103/PhysRevB.8.1346.
[60] A.A. Kornyshev, A.I. Rubinshtein, M.A. Vorotyntsev, Model nonlocal electrostatics: I, J. Phys. C 11 (1978) 3307–3322, https://doi.org/10.1088/0022-3719/11/15/029.
[61] P.J. Feibelman, Surface electromagnetic fields, Prog. Surf. Sci. 12 (1982) 287–408, https://doi.org/10.1016/0079-6816(82)90001-6.
[62] A. Kiejna, K.F. Wojciechowski, Metal Surface Electron Physics, Pergamon Press, Oxford, 1996.
[63] M.A. Vorotyntsev, A.A. Kornyshev, Electrostatics of Media with Spatial Dispersion, Nauka, Moscow, 1993 in Russian.
[64] T. Nakamura, Modification of the image potential for the interfacial zone with varying dielectric constant, J. Phys. Soc. Jpn. 52 (1983) 973–980, https://doi.org/10.1143/JPSJ.52.973.
[65] I.N. Yakovkin, Atomic wires on furrowed transition metal surfaces, J. Nanosci. Nanotechnol. 1 (2001) 357–374, https://doi.org/10.1166/jnn.2001.060.
[66] E. Bertel, E. Doná, Fermi surface tuning in two-dimensional surface systems, J. Phys. Condens. Matter 19 (2007) 355006, https://doi.org/10.1088/0953-8984/19/35/355006.
[67] I.S. Gradshteyn, I.M. Ryzhik (Eds.), Table of Integrals, Series and Products, Academic Press, San Diego, CA, 2000.
[68] Yu Z. Kovdrya, One- and zero-dimensional electron systems over liquid helium (Review Article), Fiz. Nizk. Temp. 29 (2003) 107–144, 10.1063/1.1542406] [Low Temp. Phys. 29 (2003) 77–104].
[69] C.E. Chase, E. Maxwell, The dielectric constant of liquid helium, Physica 27 (1961) 1129–1145, https://doi.org/10.1016/0031-8914(61)90054-4.
[70] J.J. Niemela, R.J. Donnelly, Density and thermal expansion coefficient of liquid helium-4 from measurements of the dielectric constant, J. Low Temp. Phys. 98 (1995) 363–421, https://doi.org/10.1007/BF00754064.
[71] B. Han, C. Robert, E. Courtade, M. Manca, S. Shree, T. Amand, P. Renucci, T. Taniguchi, K. Watanabe, X. Marie, L.E. Golub, M.M. Glazov, B. Urbaszek, Exciton states in monolayer $MoSe_2$ and $MoTe_2$ probed by upconversion spectroscopy, Phys. Rev. X 8 (2018) 31073, https://doi.org/10.1103/PhysRevX.8.031073.
[72] L.C. Gomes, P.E. Trevisanutt, A. Carvalho, A.S. Rodin, A.H. Castro Neto, Strongly bound Mott-Wannier excitons in GeS and GeSe monolayers, Phys. Rev. B 94 (2016) 155428, https://doi.org/10.1103/PhysRevB.94.155428.
[73] L.S.R. Cavalcante, A. Chaves, B. Van Duppen, F.M. Peeters, D.R. Reichman, Electrostatics of electron-hole interactions in van der Waals heterostructures, Phys. Rev. B 97 (2018) 125427, https://doi.org/10.1103/PhysRevB.97.125427.
[74] Y. Cho, T.C. Berkelbach, Environmentally sensitive theory of electronic and optical transitions in atomically thin semiconductors, Phys. Rev. B 97 (2018) 41409, https://doi.org/10.1103/PhysRevB.97.041409.
[75] P. Barcellona, R. Bennett, S.Y. Buhmann, Manipulating the Coulomb interaction: a Green's function perspective, J. Phys. Commun. 2 (2018) 35027, https://doi.org/10.1088/2399-6528/aaa70a.
[76] N.S. Rytova, Screened potential of a charge in a thin film, Vestn. Mosk. Univ. N3 (1967) 30–37.
[77] O. Manasreh, Semiconductor Heterojunctions and Nanostructures, McGraw-Hill, New York, 2005.